

# Specific Features of Amorphous Silicon Layers Grown by Plasma-Enhanced Chemical Vapor Deposition with Tetrafluorosilane

J. S. Vainshtein<sup>†</sup>, O. I. Kon'kov, A. V. Kukin, O. S. El'tsina, L. V. Belyakov,  
E. I. Terukov, and O. M. Sreseli

Ioffe Physical Technical Institute, Russian Academy of Sciences, St. Petersburg, 194021 Russia

<sup>†</sup>e-mail: julvain@gmail.com

Submitted June 24, 2010; accepted for publication July 2, 2010

**Abstract**—Hydrogenated amorphous silicon layers with crystalline nanoparticles have been produced by plasma-enhanced chemical vapor deposition, with tetrafluorosilane added to the gas mixture. The photoluminescence kinetics and photoelectric properties of structures based on these layers have been studied. The structures have a substantial photoresponse efficiency in the visible spectral range, with the position of the photoresponse maximum dependent on the applied bias.

**DOI:** 10.1134/S1063782611030225

## 1. INTRODUCTION

Nanocrystalline silicon and structures based on this material are of considerable interest as objects of study owing, first, to the manifestation of quantum-confinement effects in their properties [1] and, second, to the fact that silicon is the basis of modern microelectronics. Various methods for synthesis of silicon nanocrystallites (*nc*-Si) are being developed and studied. The following requirements are imposed upon these techniques:

- (i) a technique should enable control over the size of *nc*-Si and distances between these nanocrystallites;
- (ii) since the properties of *nc*-Si are determined not only by the size of nanocrystallites, but also, to a great extent, by the state of the *nc*-Si surface, the choice of the host medium, commonly a dielectric matrix of varied nature, is important; and
- (iii) the method should be comparatively inexpensive and possess a high output capacity and reproducibility.

These conditions are satisfied by the method of plasma-enhanced chemical vapor deposition (PECVD). This method is widely used to obtain various silicon layers: crystalline, polycrystalline, amorphous, and nanocrystalline [2–4]. Silane and hydrogen serve as starting substances in the PECVD technique. Addition of halogenosilanes to the starting mixture enables deposition of nanostructured silicon layers [5]. Silicon layers have been deposited from a mixture of tetrafluorosilane with hydrogen; it was shown that these layers contain both an amorphous phase and a crystalline phase in the form of *nc*-Si nanocrystallites 6–9 nm in size, which exhibit high-intensity photoluminescence (PL) at 1.39 eV (890 nm) [6].

In this study, we examined layers of hydrogenated amorphous silicon *a*-Si:H, deposited by PECVD from a mixture of silane and tetrafluorosilane in the atmosphere of argon and hydrogen, in order to determine the effect of fluorine ions on the structure, PL spectra, and electrical and photoelectric properties of the amorphous layers. It is shown that even a minor addition of SiF<sub>4</sub> results in silicon nanocrystals appearing in a layer.

## 2. PROCEDURE FOR FABRICATION OF LAYERS AND STRUCTURES BASED ON THESE LAYERS

Films with a thickness of 0.5 μm were deposited by decomposition of a mixture of silane, argon, hydrogen, and tetrafluorosilane in a high-frequency glow discharge plasma (PECVD) at a substrate (quartz, silicon) temperature of 220°C. The relative contents of the gases in the reaction mixture were 5% SiH<sub>4</sub>, 25% Ar, 60% H<sub>2</sub>, and 10% SiF<sub>4</sub>.

Information on the structure of the films was obtained by means of X-ray diffraction analysis, which demonstrated that amorphous films of hydrogenated silicon contain nanocrystalline inclusions with a characteristic size of 3–4 nm (*a*-Si:H + *nc*-Si films).

To perform photoelectric and electrical studies, we deposited a gold contact in the form of a grid onto the surface of films formed on *n*-type silicon substrates with a back ohmic contact.

## 3. MEASUREMENT PROCEDURE

We studied PL spectra and electrical and photoelectric properties of films deposited on silicon substrates. The PL was excited for time-resolved mea-

surements by an ILGI-503 pulsed nitrogen laser (wavelength 337 nm, pulse width 10 ns, pulse repetition frequency 100 Hz, average power 3 mW). PL spectra were measured using an automated installation based on an MDR-2 monochromator, PhEU-79 photomultiplier, V9-5 stroboscopic voltage converter, and CAMAC digital interface.

Current-voltage ( $I-V$ ) characteristics of the  $\text{Au}/\text{a-Si:H} + \text{nc-Si}/n\text{-Si}$  structure were measured using a computerized installation with an ELYPOR-3 potentiostat.

A 150-W halogen lamp and an MDR-2 monochromator served as sources of light for measurements of photoresponse spectra. The light emerging from the exit slit of the monochromator was focused onto the sample. The photocurrent was determined from the voltage drop across a small load resistor, measured with a U2-8 selective amplifier under a reverse bias applied to the structure. The photocurrent efficiency was defined as the ratio between the number of electrons involved in the photocurrent and the number of photons absorbed in unit time.

#### 4. MEASUREMENT RESULTS AND DISCUSSION

##### 4.1. Photoluminescence from an $\text{a-Si:H} + \text{nc-Si}$ Layer

The PL spectrum of the  $\text{a-Si:H} + \text{nc-Si}$  layer has the form of a very broad band (halfwidth exceeding 200 nm) with several peaks, the most pronounced of which lie at wavelengths  $\lambda = 515$  and 560–570 nm (Fig. 1). Compared with the PL from an amorphous silicon layer produced by magnetron sputtering, the PL intensity of the  $\text{a-Si:H} + \text{nc-Si}$  layer is two orders of magnitude higher. Figure 1 shows time-resolved PL spectra. It can be seen that the peak intensities differently vary with increasing delay time. The relaxation is the slowest for the peak at  $\lambda = 565$  nm. The relaxation times are very short: no longer than 50 ns for the short-wavelength peaks and 60–70 ns for the peak at  $\lambda = 565$  nm. We believe that the enhancement of the PL from the layers we obtained is due to the appearance of silicon nanocrystallites in these layers. The fast relaxation of PL may be due to the poor passivation of the nanocrystallites with hydrogen. If we assume that the “slow” peak at  $\lambda = 565$  nm (2.18 eV) is due to the quantum-confinement effect in  $\text{nc-Si}$ , then the size of these nanocrystallites can be estimated. According to [7], such an energy gap width corresponds to a crystallite size of 2.6 nm. This value correlates with X-ray diffraction data.

##### 4.2. Photoresponse of the $\text{Au}/\text{a-Si:H} + \text{nc-Si}/n\text{-Si}$ Structure

The structure under study has the form of series-connected  $\text{a-Si:H} + \text{nc-Si}$  layer and a heterojunction at the interface between the layer and single-crystalline silicon. The  $I-V$  characteristic of the structure

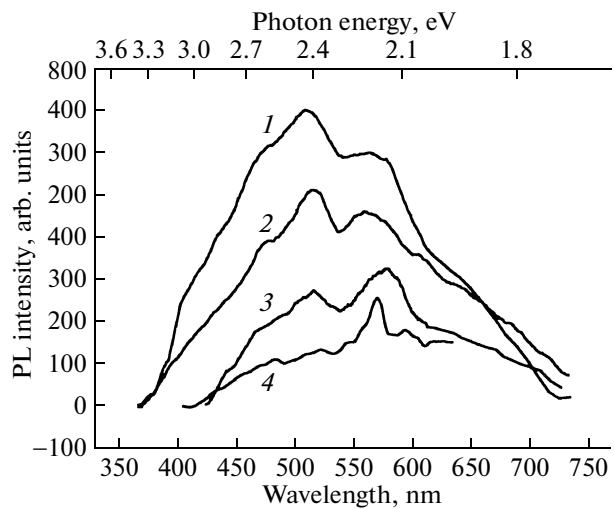


**Fig. 1.** PL spectra of an  $\text{a-Si:H} + \text{nc-Si}$  layer at different delays between the arrival of a laser pulse and signal recording: (1) 0, (2) 150, (3) 250, and (4) 350 ns. Scale of the spectra: (1)  $\times 1$ , (2)  $\times 4$ , (3)  $\times 25$ , and (4)  $\times 125$ .

exhibits a rectifying behavior, with the positive bias at the gold contact corresponding to the forward direction (Fig. 2a). The forward  $I-V$  characteristic has a turn-on voltage of  $\sim 0.4$  V. On the semilog scale, the forward characteristic is linearized at small voltages (see inset in Fig. 2a), with deviations from the straight line at voltages exceeding 0.6 V not accounted for by an increase in the voltage drop on the ohmic series resistance.

The reverse  $I-V$  characteristics shows no leveling off; the current increases with the reverse bias, which is typical of wide-gap semiconductors (Fig. 2b).

The photocurrent efficiency spectra of the  $\text{Au}/\text{a-Si:H} + \text{nc-Si}/n\text{-Si}$  structure, measured at different reverse biases, are presented in Fig. 3. The spectra show a peak in the high-energy part of the spectrum, and this peak shifts to longer wavelengths, from 2.8 to 2.4 eV, with increasing bias. In the spectral range corresponding to the absorption in the  $n\text{-Si}$  substrate, only a shoulder is observed in the photocurrent spectrum. Thus, despite the comparatively small thickness of the  $\text{a-Si:H} + \text{nc-Si}$  layer, it is this layer that makes the main contribution to the photocurrent in the structure.

Similarly to the PL spectrum, the photocurrent spectrum reflects the complex composition of the layer (Figs. 1, 3). We believe that the  $\text{a-Si:H}$  layer serves as a dielectric host for silicon nanocrystallites embedded in it.

The presence of several peaks in the PL spectrum can be interpreted as existence of several characteristic nanocrystallite sizes, instead of the common Gaussian size distribution. This behavior is occasionally observed in syntheses of nanoporous silicon [8], but it has not been unambiguously explained so far.

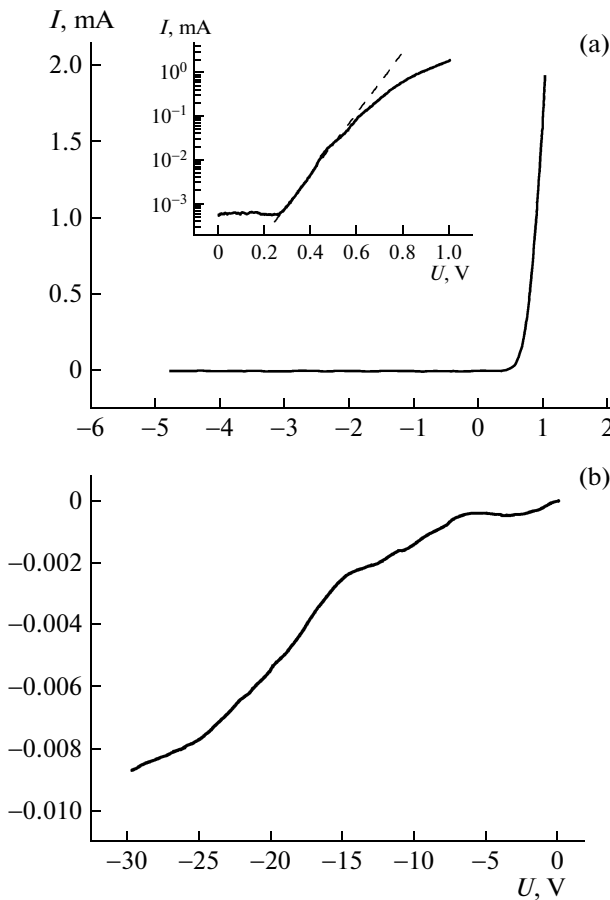


**Fig. 2.** (a)  $I$ - $V$  characteristics of the  $\text{Au}/\text{a-Si:H} + \text{nc-Si}/\text{n-Si}$  structure. Inset: forward  $I$ - $V$  characteristic plotted on the semilog scale. (b) Reverse  $I$ - $V$  characteristic.

The shift of the peak in the photocurrent efficiency spectrum with increasing reverse bias can also be attributed to presence of silicon crystallites with different sizes. Let us assume that, in the course of layer deposition onto a substrate, the finest crystallites are situated close to the heterojunction and, as the  $\text{a-Si:H} + \text{nc-Si}$  layer grows, increasingly coarse nanocrystallites are formed. Then, as the applied bias is raised, crystallites increasingly remote from the junction, which are coarser in our case, start to be involved in the photocurrent; it is this circumstance that leads to a shift of the spectral peak to lower energies.

We were also interested in the photoresponse of a layer with Si nanocrystallites in the far-UV spectral range, in which impact ionization and carrier multiplication at quantum dots (nanocrystallites) are known [9, 10] to be possible upon absorption of photons with energies more than twice exceeding the effective width of the energy gap ( $E_g$ ) in quantum dots. The photoresponse efficiency spectra in the UV spectral range (up to 4.2 eV) are shown in Fig. 4. Beginning at approximately 2.8 eV, the efficiency sharply falls, because incident photons are absorbed near the sur-

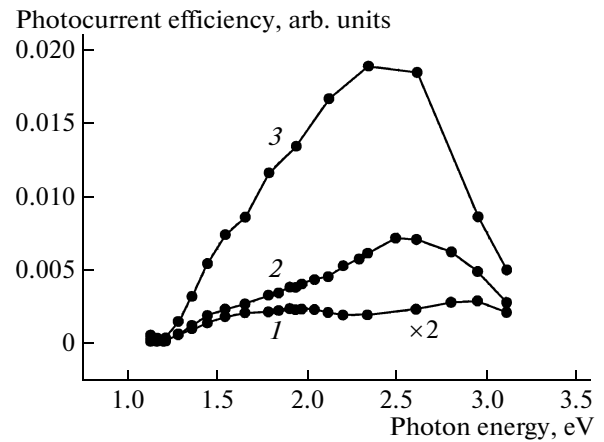


**Fig. 3.** Photoresponse spectra of the structures at the following reverse voltages: (1) 3, (2) 9, and (3) 18 V.

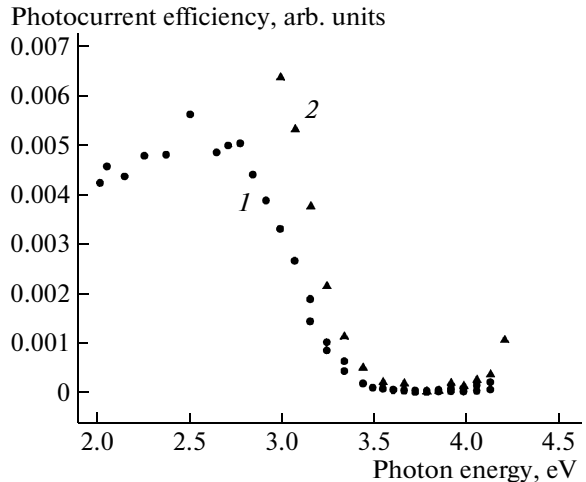


**Fig. 4.** Photoresponse spectra of the structures in the short-wavelength spectral range at different reverse voltages: (1) 3 and (2) 9 V.

face layer and carriers they generate cannot reach the heterojunction.

In other words, at photon energies higher than 3.5 eV, only a weak signal of the photoconductivity in the  $\text{a-Si:H} + \text{nc-Si}$  layer manifests itself in the photoresponse. A certain rise in the photocurrent efficiency is observed in the high-energy part of the spectrum, beginning at 3.9–4.0 eV. However, this signal is weak; therefore, we cannot unambiguously attribute this rise to impact ionization of carriers. Since most of nanocrystallites have an effective  $E_g$  within the range 2.4–2.8 eV, a strong signal caused by impact ionization must be observed at photon energies higher than 5 eV. At the same time, our results suggest that further efforts aimed at optimization of the layer composition and development of the technology to improve the passivation of nanocrystallites and raise their size will

result in a substantial increase in the photocurrent efficiency in the UV spectral range.

## 5. CONCLUSIONS

It was demonstrated that addition of trifluorosilane to the gas mixture in deposition of  $\alpha$ -Si:H layers by the PECVD method results in silicon nanocrystallites with sizes smaller than  $3\text{ }\mu\text{m}$  being formed in a layer.

Layers of this kind are characterized by photoluminescence in a wide spectral range, with peaks shifted to shorter wavelengths in accordance with the nanocrystallite sizes.

The photoresponse efficiency of the Au/ $\alpha$ -Si:H +  $nc$ -Si/ $n$ -Si structures fabricated in this study is mostly determined by the absorption of light in the  $\alpha$ -Si:H +  $nc$ -Si layer and strongly depends on the applied bias.

The layers obtained are of interest for use in thin-film solar cells.

## ACKNOWLEDGMENTS

The study was supported by the Russian Foundation for Basic Research (projects nos. 10-02-00828 and 07-08-92163-NTsNI-a) and the Presidential Grant of the Russian Federation in Support of Leading Scientific Schools (NSh 3306.20102).

## REFERENCES

1. A. G. Gullis, L. T. Canham, and P. D. J. Calcott, *J. Appl. Phys.* **82**, 909 (1997).
2. S. V. Chernyshov, E. I. Terukov, V. A. Vassilyev, and A. S. Volkov, *J. Non.-Cryst. Solid* **134**, 218 (1991).
3. A. Hadded-Adel, T. Inokuma, Y. Kurata, and S. Hasegawa, *Surf. Sci.* **601**, 1429 (2007).
4. T. Nagahara, K. Fujimoto, N. Kohno, K. Kashiwagi, and H. Kakinoki, *Jpn. J. Appl. Phys.* **31**, 4555 (1992).
5. M. Lozurdo, M. M. Giangregorio, A. Sacchetti, P. Capuzzuto, G. Bruno, J. Cárabe, J. J. Ganda, and L. Urbina, *J. Non.-Cryst. Solid* **352**, 906 (2006).
6. P. G. Sennikov, S. V. Golubev, V. I. Shashkin, D. A. Pryakhin, M. N. Drozdov, B. A. Andreev, Yu. N. Drozdov, A. S. Kuznetsov, and Kh.-J. Pol, *Pis'ma Zh. Eksp. Teor. Fiz.* **89** (2), 86 (2009) [JETP Lett. **89**, 73 (2009)].
7. C. Delerue, G. Allan, and M. Lannoo, *J. Luminesc.* **80**, 65 (1999).
8. V. Osinniy, S. Lesgaard, V. Kolkovsky, V. Pankratov, and A. Nylandsted Larsen, *Nanotechnology* **20**, 195201 (2009).
9. D. Timmerman, I. Izeddin, P. Stallinga, I. N. Yassievich, and T. Gregorkiewicz, *Nature Photon.* **2**, 105 (2008).
10. O. M. Sreeseli, O. S. El'tsina, L. V. Belyakov, and D. N. Gorychev, *Appl. Phys. Lett.* **95**, 031914 (2009).

*Translated by M. Tagirdzhanov*